

Measurement of dipole matrix elements with a single trapped ion

M. Hettrich,^{1,*} T. Ruster,¹ H. Kaufmann,¹ C. F. Roos,^{2,3} C. T. Schmiegelow,¹ F. Schmidt-Kaler,¹ and U. G. Poschinger¹

¹QUANTUM, Institut für Physik, Universität Mainz, Staudingerweg 7, 55128 Mainz, Germany[†]

²Institut für Quantenoptik und Quanteninformation, Österreichische Akademie der Wissenschaften, Technikerstraße 21a, 6020 Innsbruck, Austria

³Institut für Experimentalphysik, Universität Innsbruck, Technikerstraße 25, 6020 Innsbruck, Austria

(Dated: March 27, 2025)

We demonstrate a new method for the direct measurement of atomic dipole transition matrix elements based on techniques developed for quantum information purposes. The scheme consists of measuring dispersive and absorptive off-resonant light-ion interactions and is applicable to many atomic species. We determine the dipole matrix element pertaining to the Ca II H line, i.e. the $4^2S_{1/2} \leftrightarrow 4^2P_{1/2}$ transition of $^{40}\text{Ca}^+$, for which we find the value $2.893(8) \text{ ea}_0$. Moreover, the method allows us to deduce the lifetime of the $4^2P_{1/2}$ state to be $6.90(5) \text{ ns}$, which is in agreement with predictions from recent theoretical calculations and resolves a longstanding discrepancy between calculated values and experimental results.

PACS numbers: 37.10.Ty, 37.10.-x, 32.80.Qk, 03.67.Lx

Methods for trapping and cooling single or few atoms, molecules or ions and manipulating them at the quantum level have opened up new avenues for precision laser spectroscopy. In particular, quantum logic techniques [1] have enabled a new accuracy regime of timekeeping with optical atomic clocks [2]. In contrast to atomic transition frequencies, dipole matrix elements and radiative lifetimes are still notoriously hard to measure at high precision. The accurate and precise determination of these quantities is of importance for the quantification of black body radiation shifts of atomic clocks [3], interpretation of astrophysical spectra [4, 5], novel approaches for the search for physics beyond standard model [6, 7] and for testing the accuracy of atomic structure calculations [8]. For the measurement of radiative lifetimes and transition matrix elements, established methods e.g. based on ion beams have been successfully complemented by novel techniques based on trapped particles. For ^{87}Rb , dipole matrix elements have been determined on the 10^{-3} accuracy level by diffraction in a condensate [9], while for the $6p^2P_{1/2}^O$ state of $^{174}\text{Yb}^+$, the radiative lifetime has been measured by time-resolved counting of photons emitted from a single trapped ion [10]. A related technique was used for neutral ^{171}Yb in an optical lattice [11]. The species Ca^+ is widely used in quantum optics experiments, and its II H line led to the discovery of the interstellar medium [12]. For $^{40}\text{Ca}^+$, branching ratios between different decay channels have been determined at accuracies approaching the 10^{-5} level [13, 14], and lifetimes of metastable states have been accurately measured [15]. The $4^2P_{1/2}$ radiative lifetime has been determined to be $7.098(20) \text{ ns}$ [16] by fluorescence measurements on a fast ion beam. However, this value deviates by more than 11 standard deviations from the most recent theoretical calculation [8], while similar calculations for alkaline-like species from Li to Fr, Mg^+ , Ba^+ and Sr^+ are in good

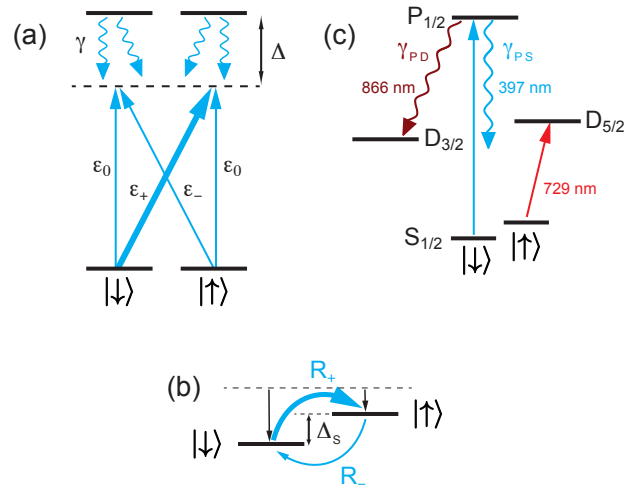


FIG. 1. (color online) Measurement scheme: (a) a laser off-resonantly couples two Zeeman ground state levels to an excited state with decay rate γ . (b) The coupling gives rise to a differential ac-Stark shift Δ_S between the Zeeman levels and incoherent redistribution of population at rates R_{\pm} . (c) Relevant energy levels in $^{40}\text{Ca}^+$. The shelving to the metastable $3^2D_{5/2}$ state as well the $3^2D_{3/2}$ state acting as a population sink are indicated.

agreement with experimental results (see [8] and references therein). In this work, we present a measurement of the radiative decay rates of the $4^2P_{1/2}$ excited state of $^{40}\text{Ca}^+$. It is based on techniques used for preparation, coherent manipulation and read-out of atomic states developed for ion trap quantum computing [17, 18]. As our scheme works with a single trapped ion and discrete discrimination of atomic states rather than temporal or spatial quantification of resonance fluorescence counts, it is robust against many systematic error sources which affect other existing methods. Our method allows for the determination of one specific matrix element even in the

presence of other decay channels, and it is applicable to atom and ion species which allow for preparation and readout of Zeeman or hyperfine sublevels.

The cornerstone of the method is the comparison between *dispersive* and *absorptive* interaction of a single $^{40}\text{Ca}^+$ ion with an off-resonant laser beam, which provides dipolar coupling of the $4^2\text{S}_{1/2}$ ground state to the $4^2\text{P}_{1/2}$ excited state. The laser electric field at the position of the ion is $\mathbf{E}(t) = \sum_{q=\pm,1} \mathcal{E}\epsilon_q \mathbf{e}_q e^{-i\omega_0 t} + c.c.$, where the ϵ_q characterize the relative amplitudes of the circular ($q = \pm 1$, denoted '±' henceforth) and π ($q = 0$) polarization components, ω_0 is the optical frequency, \mathbf{e}_q are the spherical basis vectors and \mathcal{E} is the electric field amplitude. The coupling is described by the Rabi frequency $\Omega = 2\mathcal{E}\mathcal{D}/\hbar$, where $\mathcal{D} = \langle S_{1/2} || \hat{\mathbf{d}} || P_{1/2} \rangle$ is the reduced matrix element of the dipole operator. The polarization components ϵ_q drive transitions between Zeeman sublevels with $m_P - m_S = q$ at effective Rabi frequencies scaled with the respective Wigner 3j-symbol, $\Omega\epsilon_q \begin{pmatrix} 1/2 & 1 & 1/2 \\ -m_S & q & m_P \end{pmatrix}$. The radiative decay rate from the $P_{1/2}$ to the $S_{1/2}$ state, γ_{PS} , is related to \mathcal{D} by

$$\mathcal{D}^2 = 2\gamma_{PS} \frac{3\epsilon_0 \hbar}{8\pi^2} \lambda_{PS}^3, \quad (1)$$

where λ_{PS} is the resonance wavelength. The laser is detuned far from the power-broadened resonance, by a frequency $|\Delta| \gg \Omega, \gamma_{PS}$.

The *dispersive* interaction with the laser causes ac Stark shifts of the energy levels, which is exploited in atomic physics e.g. for optical trapping [19] of atoms or for quantum state manipulation of trapped ions [20, 21]. In our scheme, we are interested in the differential ac Stark shift Δ_S between the two Zeeman-sublevels of the electronic ground state $|S_{1/2}, m_S = \pm 1/2\rangle$, denoted henceforth as $|\uparrow\rangle$ and $|\downarrow\rangle$:

$$\Delta_S = \frac{1}{3} \frac{\Omega^2}{4\Delta} (\epsilon_-^2 - \epsilon_+^2), \quad (2)$$

The *absorptive* interaction manifests itself through inelastic Raman scattering, i.e. spin flips [22, 23]. R_+ denotes the spin flip rate from $|\downarrow\rangle$ to $|\uparrow\rangle$ and R_- the rate in the inverse direction respectively. For a beam with arbitrary polarization this reads [20]

$$R_{\pm} = \gamma_{PS} \frac{\epsilon_{\pm}^2 + \epsilon_0^2}{9} \frac{\Omega^2}{4\Delta^2} \quad (3)$$

Note that the π -polarized light drives the two spin-flip directions equally strong, whereas each of the the circular components drives only one pathway, corresponding to optical pumping in the limit of purely circularly polarized light. The occurrence of elastic (Rayleigh) scattering is taken into account. For population leakage by decay to the $3^2\text{D}_{3/2}$ state at rate γ_{PD} , we make the assumption that only circular components are present in the beam, i.e. $\epsilon_0^2 \approx 0$, which is justified below. Then, one out of three photon scattering events leads to a spin flip. The

rates at which population from $|\uparrow\rangle$ ($|\downarrow\rangle$) is sunk in the metastable $3^2\text{D}_{3/2}$ state are then given by

$$R_{\uparrow(\downarrow)D} = 3(\gamma_{PD}/\gamma_{PS})R_{-(+)}. \quad (4)$$

The spin-flip dynamics can then be described by the rate equations:

$$\begin{aligned} \dot{p}_{\uparrow} &= -R_-(1+b)p_{\uparrow} + R_+p_{\downarrow} \\ \dot{p}_{\downarrow} &= -R_+(1+b)p_{\downarrow} + R_-p_{\uparrow}. \end{aligned} \quad (5)$$

with the leak factor $b = 3(\gamma_{PD}/\gamma_{PS})$. The solution of Eqs. 5 is

$$\begin{aligned} \dot{p}_{\uparrow}^{(\uparrow)}(t) &= \frac{1}{\bar{R}} e^{-\frac{1}{2}\bar{R}t} \left(\tilde{R} \cosh\left(\frac{\tilde{R}t}{2}\right) - (1+b)\delta R \sinh\left(\frac{\tilde{R}t}{2}\right) \right) \\ \dot{p}_{\uparrow}^{(\downarrow)}(t) &= \frac{2}{\bar{R}} e^{-\frac{1}{2}\bar{R}t} R_+ \sinh(\tilde{R}t/2), \end{aligned} \quad (6)$$

with $p_{\uparrow}^{(\uparrow)}$ corresponding to initialization in $|\uparrow\rangle$, $p_{\uparrow}(t=0) = 1$, and $p_{\uparrow}^{(\downarrow)}$ for initialization in $|\downarrow\rangle$, $p_{\uparrow}(t=0) = 1$. We use $\bar{R} = (1+b)(R_- + R_+)$ and $\tilde{R}^2 = \bar{R}^2 - 4b(2+b)R_-R_+$. Combining Eqs. 2 and 3, the decay rate γ_{PS} reads

$$\gamma_{PS} = 3\Delta \frac{\delta R}{\Delta_S}, \quad (7)$$

with $\delta R = R_- - R_+$. All quantities on the rhs of 7 are independently experimentally accessible, which allows us to determine γ_{PS} . The Rabi frequency Ω , which is hard to determine experimentally, does not appear in that expression.

We perform measurements on a single $^{40}\text{Ca}^+$ ion stored in a segmented Paul trap [24]. The relevant energy levels and transitions are depicted in Fig. 1. The Zeeman sublevels of the electronic ground state $|\uparrow\rangle$ and $|\downarrow\rangle$ are split by $2\pi \times 13.7$ MHz. We perform Doppler cooling on the $4^2\text{S}_{1/2} \leftrightarrow 4^2\text{P}_{1/2}$ (cycling) transition near 397 nm. After cooling, the ion is prepared in either $|\uparrow\rangle$ or $|\downarrow\rangle$ by optical pumping. After the state manipulations described below, spin read-out is accomplished by shelving population from the $|\uparrow\rangle$ level to the metastable $3^2\text{D}_{5/2}$ state by means of rapid adiabatic passage (RAP) pulses [18, 25]. The ion is then illuminated by laser fields driving the cycling transition and the $3^2\text{D}_{3/2} \leftrightarrow 4^2\text{P}_{1/2}$ transition near 866 nm, such that fluorescence is detected on a photomultiplier tube if the ion is not in the metastable $3^2\text{D}_{5/2}$ state. The probability of fluorescence detection therefore corresponds to the population being in the $|\downarrow\rangle$ and $3^2\text{D}_{3/2}$ states after the manipulation. The off-resonant light near 397 nm is provided by an amplified and frequency-doubled diode laser system, stabilized in both wavelength ($\delta\Delta/\Delta \lesssim 0.5 \cdot 10^{-3}$) and intensity ($\delta I/I \lesssim 0.5 \cdot 10^{-3}$). The beam is aligned along the quantizing magnetic field and predominantly σ^+ polarized, such that $R_+ \gg R_-$, and $\epsilon_0^2 \approx 0$, justifying the approximation for Eq. 4. The measurement of the ac Stark shift Δ_S is accomplished by performing a spin-echo technique: A $\pi/2$ pulse on the stimulated Raman transition between $|\uparrow\rangle$ and $|\downarrow\rangle$

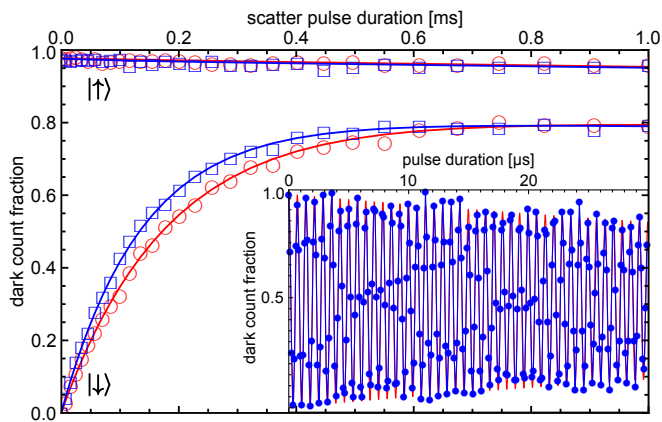


FIG. 2. (color online) Dark count fraction versus time of exposure to an off-resonant laser pulse for initializations in $|\uparrow\rangle$ and $|\downarrow\rangle$. Data points indicated by blue squares (red circles) are measured with the laser detuned by 12.03 GHz (13.94 GHz) from resonance. Solid lines show the fits to the model Eq. (6). The inset shows the dark count fraction versus pulse duration for a spin-echo experiment. The blue line connects the datapoints, the red line is the resulting fit. The oscillation frequency directly corresponds to the differential ac Stark shift Δ_S .

is followed by a π pulse, another $\pi/2$ pulse concludes the sequence. The delay time between the pulses is constant. During the first delay, the ion is exposed to an off-resonant square pulse of variable duration. We probe 250 different shift pulse times, each with 150 interrogations. The times are spaced by 120 ns, such that a signal with about 40 oscillation periods is obtained. The differential ac Stark shift is the frequency of this oscillatory dark count fraction (see inset of Fig. 2).

For the measurement of the spin-flip rates R_{\pm} , the ion is exposed to pulses of variable duration up to 1 ms of the off-resonant laser after preparation. In contrast to the ac Stark shift measurement, the required quantities are slopes rather than a frequency, thus substantially more data has to be acquired in order to reduce the impact of readout shot noise. For each measurement, the dark count fraction is determined by probing the ion 2500 times for 30 fixed scatter pulse durations. The resulting total dark count fractions versus pulse time are shown in Fig. 2. The time gap between initialization and readout is kept constant irrespectively of the scatter pulse duration to avoid systematic effects. We extract the parameters δR and b from the spin flip data by means of a Markov chain Monte Carlo parameter estimation, taking into account the binomial statistics of the quantum projection noise in the spin readout. State preparation and measurement errors are taken into account by modeling the measured dark count fractions as a linear transformation of the values $\dot{p}_{\uparrow}^{(\uparrow)}(t), p_{\uparrow}^{(\downarrow)}(t)$ from Eqs. 6.

65 independent data sets were taken, each comprised of spin flip rate measurements for preparation both in $|\uparrow\rangle$ and $|\downarrow\rangle$, and ac Stark shift measurements taken directly

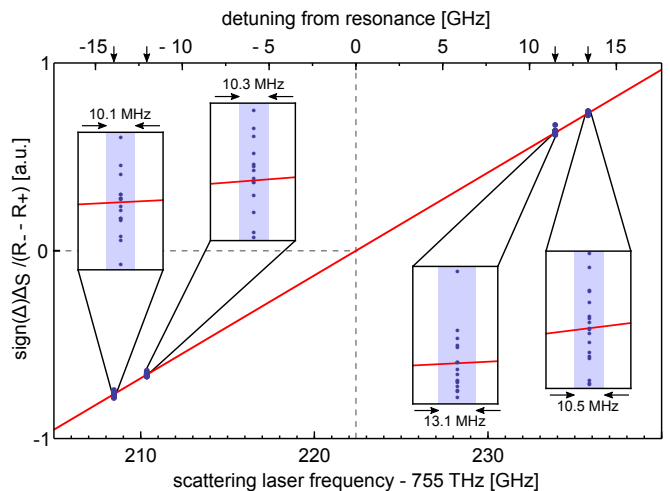


FIG. 3. (color online) Determination of the four detunings chosen for our measurements. For each of the 65 acquired datasets, we plot the quantity $\text{sign}(\Delta)\Delta_S/\delta R \propto \Delta$ versus the optical frequency as measured by a wavelength meter. The zero crossing of a linear fit, depicted by the solid red line, reveals the resonance frequency with a standard error of $2\pi \cdot 21$ MHz. The insets show details of the datasets measured at the different detunings with the abscissa magnified 166 times. The shaded backgrounds indicate their uncertainties along the frequency axis. The arrows on the top frequency scale indicate the values of the four different detunings at -13.94, -12.03, 11.52 and 13.42 GHz.

before and after the spin flip measurements in order to capture drifts of the laser intensity and thus the Rabi frequency Ω . The total data acquisition time was about 50 h. The acquired data sets are taken for four different laser detunings. To determine the value of these detunings, we read the optical frequency from a commercial wavelength meter (High Finesse WSU 267) with better than 10 MHz precision. We perform a linear regression of the measured Δ_S divided by δR versus the corresponding optical frequencies to obtain the resonance frequency, as shown in Fig. 3. Compared to direct fluorescence spectroscopy, this technique mitigates effects like power broadening, Zeeman splitting micro motion-induced broadening, which would make a determination of the resonance frequency less accurate.

We combine the measured quantities Δ, Δ_S and δR , using Eq. 7, to obtain the desired value γ_{PS} . Together with b this also yields $\gamma_{PD} = \frac{b}{3}\gamma_{PS}$. The radiative lifetime is given by $1/\tau = \gamma_{PS}(1 + \frac{b}{3})$. Averaging over the data sets and taking into account the corrections discussed below, we obtain the resulting values: $\gamma_{PS} = 2\pi \times 21.57(15)$ MHz and a $4^2P_{1/2} \rightarrow 4^2S_{1/2}$ branching fraction of $1/(1 + \frac{b}{3}) = 0.9357(4)$. This leads to a lifetime of $\tau = 6.90(5)$ ns and a value of $\gamma_{PD} = 2\pi \times 1.481(15)$ MHz. Together with the absolute wavelength λ_{PS} of the $4^2S_{1/2} \leftrightarrow 4^2P_{1/2}$ transition, we obtain the reduced matrix element \mathcal{D} of the respective transition as well, using Eq. 1. We determine a

value of $\mathcal{D} = 2.893(8) \text{ ea}_0$. Experimental imperfections and model approximations lead to errors and corrections for the value of γ_{PS} . These are summarized in Table I: Beyond the approximation in Eq. 4, a possible ϵ_0 polarization component has been taken into account, and yields corrections and systematic errors on the 10^{-3} level. The precision of the detuning Δ is limited by the wavelength meter, and its accuracy is limited by the determination of the resonance frequency. Statistical uncertainties of the measurement values δR and b , determined by the amount of acquired data, represent a major contribution to the error budget. Residual resonant light close to 397 nm resulting from imperfect laser switch-off causes relative corrections and systematic errors in the 10^{-4} regime. Beyond the rate equation model Eq. 5, we include a correction for the finite lifetime of the $3^2D_{3/2}$ state or its depletion by residual light near 866 nm. Δ_S can be measured by orders of magnitude more precisely than δR and b , however the precision is limited by drift effects, quantified by monitoring the ac Stark shift over the entire data acquisition time. Excess micromotion of the ion also causes a small systematic error via frequency modulation of the off-resonant light. Furthermore, we include corrections due to the presence of the $4^2P_{3/2}$ state about $2\pi \times 6.69$ THz above the $4^2P_{1/2}$ state, and due to the power-broadened Lorentzian lineshape beyond the assumption $|\Delta| \gg \Omega, \gamma_{PS}$. A detailed discussion of corrections and errors is presented in the supplemental material [?].

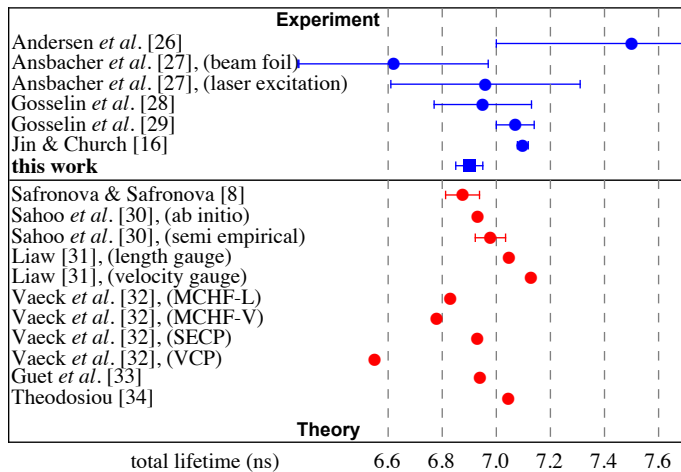


FIG. 4. Comparison of the measured lifetime with theoretical and experimental results for $P_{1/2}$ - level lifetimes from references [8, 16, 26, 27, 28, 29, 30, 31, 32, 33, 34]

Our value for τ is compared to previously reported values in Fig. 4. We find that our value agrees with the latest theory predictions [8], while it is in substantial disagreement with the most recent experimental result [16]. Our value for the branching fraction is in agreement with the results from recent measurements [14]. To our knowledge

TABLE I. List of relative measurement uncertainties for γ_{PS} . Statistical errors are denoted by (*). The shift for the $P_{3/2}$ state depends on Δ , we indicate the average value here. Note that the total error is not the sum of the individual contributions, as statistical and systematic errors are taken into account.

Effect	Shift $\cdot 10^{-3}$	Error $\cdot 10^{-3}$
Residual ϵ_0 polarized light	3.3	2.9
Uncert. of resonance frequency	-	1.6
Stat. uncertainty of δR	-	1.3(*)
Residual near-resonant light	-0.4	0.5
Wavemeter precision	-	0.4(*)
$D_{3/2}$ depletion	0.3	0.2
Uncertainty of Δ_S	-	0.2(*)
Influence of micro motion	-	0.1
Influence of $P_{3/2}$ state	0.3	< 0.1
Residual line-broadening effects	0.1	< 0.1
Total	+3.6	6.8

there is no experimentally determined value of \mathcal{D} so far, where our value is in agreement with the calculation from [8] as well. It is possible to infer the value of the reduced matrix element pertaining to the $4^2S_{1/2} \leftrightarrow 4^2P_{3/2}$ transition, which results to $\sqrt{2}\mathcal{D} = 4.09(1) \text{ ea}_0$. Both reduced dipole matrix elements enter in the calculation of the blackbody-radiation (BBR) shift of the $4^2S_{1/2} \leftrightarrow 3^2D_{3/2}$ and $4^2S_{1/2} \leftrightarrow 3^2D_{5/2}$ quadrupole transitions, which are widely used testbeds for high precision laser spectroscopy [35]. The BBR shift is a major contributor to the uncertainty of clock transition frequencies, for species such as $^{43}\text{Ca}^+$ [36], Al^+ [37] and Sr [38], some of which are used for state-of-the art optical clock experiments and discussed as new SI frequency standards [1, 39, 40]. Our results confirm the validity of computational methods used to predict the BBR shift in such optical clocks. In summary, we demonstrate a novel method for the measurement of dipole matrix elements, which relies on quantum logic techniques and which works in the presence of additional decay channels. We attain a precision and accuracy on the 10^{-3} level. All major error sources can be potentially mitigated, such that measurements of radiative decay rates at unprecedented accuracies in the 10^{-4} regime appear within reach with current technology.

We acknowledge financial support by the European commission within the IP SIQS and by the Bundesministerium für Bildung und Forschung via IKT 2020 (Q.com). We thank Vladan Vuletic, Rene Gerritsma and Marianna Safronova for helpful discussions.

* hettrich@uni-mainz.de

† <http://www.quantenbit.de>

[1] P. O. Schmidt, T. Rosenband, C. Langer, W. M. Itano, J. C. Bergquist, and D. J. Wineland, *Science*, **309**, 749 (2005)

- [2] T. Rosenband, D. B. Hume, P. O. Schmidt, C. W. Chou, A. Brusch, L. Lorini, W. H. Oskay, R. E. Drullinger, T. M. Fortier, J. E. Stalnaker, S. A. Diddams, W. C. Swann, N. R. Newbury, W. M. Itano, D. J. Wineland, and J. C. Bergquist, *Science*, **319**, 1808 (2008)
- [3] M. S. Safronova, M. G. Kozlov, and C. W. Clark, *Phys. Rev. Lett.*, **107**, 143006 (2011)
- [4] E. Rauscher and G. W. Marcy, *PASP*, **118**, 617 (2006)
- [5] M. Carlsson and J. Leenaarts, *A&A*, **539**, A39 (2012)
- [6] N. Fortson, *Phys. Rev. Lett.*, **70**, 2383 (1993)
- [7] T. W. Koerber, M. H. Schacht, K. R. G. Hendrickson, W. Nagourney, and E. N. Fortson, *Phys. Rev. Lett.*, **88**, 143002 (2002)
- [8] M. S. Safronova and U. I. Safronova, *Phys. Rev. A*, **83**, 012503 (2011)
- [9] C. D. Herold, V. D. Vaidya, X. Li, S. L. Rolston, J. V. Porto, and M. S. Safronova, *Phys. Rev. Lett.*, **109**, 243003 (2012)
- [10] S. Olmschenk, D. Hayes, D. N. Matsukevich, P. Maunz, D. L. Moehring, K. C. Younge, and C. Monroe, *Phys. Rev. A*, **80**, 022502 (2009)
- [11] K. Beloy, J. A. Sherman, N. D. Lemke, N. Hinkley, C. W. Oates, and A. D. Ludlow, *Phys. Rev. A*, **86**, 051404 (2012)
- [12] J. Hartmann, *Astrophysical Journal*, **19**, 268 (1904)
- [13] R. Gerritsma, G. Kirchmair, F. Zähringer, J. Benhelm, R. Blatt, and C. F. Roos, *Eur. Phys. J. D*, **50**, 13 (2008)
- [14] M. Ramm, T. Pruttivarasin, M. Kokish, I. Talukdar, and H. Häffner, *Phys. Rev. Lett.*, **111**, 023004 (2013)
- [15] A. Kreuter, C. Becher, G. P. T. Lancaster, A. B. Mundt, C. Russo, H. Häffner, C. Roos, W. Hänsel, F. Schmidt-Kaler, R. Blatt, and M. S. Safronova, *Phys. Rev. A*, **71**, 032504 (2005)
- [16] J. Jin and D. A. Church, *Phys. Rev. Lett.*, **70**, 3213 (1993)
- [17] D. Leibfried, R. Blatt, C. Monroe, and D. Wineland, *Rev. Mod. Phys.*, **75**, 281 (2003)
- [18] U. G. Poschinger, G. Huber, F. Ziesel, M. Deiss, M. Hettrich, S. A. Schulz, G. Poulsen, M. Drewsen, R. J. Hendricks, K. Singer, and F. Schmidt-Kaler, *J. Phys. B: At. Mol. Opt. Phys.*, **42**, 154013 (2009)
- [19] R. Grimm and M. Weidemüller, *Adv. At. Mol. Opt. Phys.*, **42**, 95 (2000)
- [20] D. J. Wineland, M. Barret, J. Britton, J. Chiaverini, B. DeMarco, W. M. Itano, B. Jelenkovic, C. Langer, D. Leibfried, V. Meyer, T. Rosenband, and T. Schätz, *Phil. Trans. R. Soc. Lond. A.*, **361**, 1349 (2003)
- [21] D. Leibfried, B. DeMarco, V. Meyer, D. Lucas, M. Barrett, J. Britton, W. M. Itano, B. Jelenkovic, C. Langer, T. Rosenband, and D. J. Wineland, *Nature*, **422**, 412 (2003)
- [22] R. Ozeri, C. Langer, J. D. Jost, B. DeMarco, A. Ben-Kish, B. R. Blakestad, J. Britton, J. Chiaverini, W. M. Itano, D. B. Hume, D. Leibfried, T. Rosenband, P. O. Schmidt, and D. J. Wineland, *Phys. Rev. Lett.*, **95**, 030403 (2005)
- [23] H. Uys, M. J. Biercuk, A. P. VanDevender, C. Ospelkaus, D. Meiser, R. Ozeri, and J. J. Bollinger, *Phys. Rev. Lett.*, **105**, 200401 (2010)
- [24] S. Schulz, U. Poschinger, F. Ziesel, and F. Schmidt-Kaler, *New J. Phys.*, **10**, 045007 (2008)
- [25] C. Wunderlich, T. K. Th. Hannemann and, H. Häffner, C. Roos, W. Hänsel, R. Blatt, and F. Schmidt-Kaler, *J. Mod. Opt.*, **54**, 1541 (2007)
- [26] T. Andersen, J. Desesquelles, K. A. Jessen, and G. Sørensen, *J. Quant. Spectrosc. Radiat. Transfer*, **10**, 1143 (1970)
- [27] W. Ansbacher, A. S. Inamdar, and E. H. Pinnington, *Phys. Lett.*, **110A**, 383 (1985)
- [28] R. N. Gosselin, E. H. Pinnington, and W. Ansbacher, *Nuc. Inst. Meth. B*, **31**, 305 (1988)
- [29] R. N. Gosselin, E. H. Pinnington, and W. Ansbacher, *Phys. Rev. A*, **38**, 4887 (1988)
- [30] B. K. Sahoo, B. P. Das, and D. Mukherjee, *Phys. Rev. A*, **79**, 052511 (2009)
- [31] S.-S. Liaw, *Phys. Rev. A*, **51**, R1723 (1995)
- [32] N. Vaeck, M. Godefroid, and C. Froese Fischer, *Phys. Rev. A*, **46**, 3704 (1992)
- [33] C. Guet and W. R. Johnson, *Phys. Rev. A*, **44**, 1531 (1991)
- [34] C. E. Theodosiou, *Phys. Rev. A*, **39**, 4880 (1989)
- [35] M. Chwalla, J. Benhelm, K. Kim, G. Kirchmair, T. Monz, M. Riebe, P. Schindler, A. S. Villar, W. Hänsel, C. F. Roos, R. Blatt, M. Abgrall, G. Santarelli, G. D. Rovera, and P. Laurent, *Phys. Rev. Lett.*, **102**, 023002 (2009)
- [36] B. Arora, M. S. Safronova, and C. W. Clark, *Phys. Rev. A*, **76**, 064501 (2007)
- [37] M. S. Safronova, M. G. Kozlov, and C. W. Clark, *IEEE Transactions on Ultrasonics, Ferroelectrics, and Frequency Control*, **59**, 439 (2012)
- [38] M. S. Safronova, S. G. Porsev, U. I. Safronova, M. G. Kozlov, and C. W. Clark, *Phys. Rev. A*, **87**, 012509 (2013)
- [39] C. W. Chou, D. B. Hume, J. C. J. Koelemeij, D. J. Wineland, and T. Rosenband, *Phys. Rev. Lett.*, **104**, 070802 (2010)
- [40] B. J. Bloom, T. L. Nicholson, J. R. Williams, S. L. Campbell, M. Bishof, X. Zhang, W. Zhang, S. L. Bromley, and J. Ye, *Nature*, **506**, 71 (2014)